27. De Sandre-Giovannoli, A. *et al.* Homozygous defects in *LMNA*, encoding lamin A/C nuclear-envelope proteins, cause autosomal recessive axonal neuropathy in human (Charcot-Marie-Tooth disorder type 2) and mouse. *Am. J. Hum. Genet.* **70,** 726–736 (2002).
28. Speckman, R. A. *et al.* Mutational and haplotype analyses of families with familial partial lipodystrophy (Dunnigan variety) reveal recurrent missense mutations in the globular C-terminal domain of lamin A/C. *Am. J. Hum. Genet.* **66,** 1192–1198 (2000); erratum **67,** 775 (2000).

Supplementary Information accompanies the paper on **www.nature.com/nature**.

Acknowledgements We are grateful to all of the families with HGPS who donated blood and skin samples, without which this study would not have been possible. We would also like to express our gratitude to the entire Progeria Research Consortium, especially B. Toole, for their encouragement during the course of this work. We also thank E. Gillanders for providing the linkage marker set; P. Hollstein for assistance with genotyping; P. Chines for the identification of additional microsatellite markers on chromosome 1q; and M. Kirby for assistance with the flow cytometry. Support from the Progeria Research Foundation (L.B.G., M.W.G. and T.W.G.) and the Bedminster Foundation (W.T.B.) is gratefully acknowledged.

Competing interests statement The authors declare that they have no competing financial interests.

Correspondence and requests for materials should be addressed to F.S.C. (fc23a@nih.gov).

A progeroid syndrome in mice is caused by defects in A-type lamins

Leslie C. Mounkes, Serguei Kozlov, Lidia Hernandez, Teresa Sullivan & Colin L. Stewart

Cancer and Developmental Biology Laboratory, National Cancer Institute, Frederick, Maryland 21702, USA

Numerous studies of the underlying causes of ageing have been attempted by examining diseases associated with premature ageing, such as Werner's syndrome and Hutchinson–Gilford progeria syndrome (HGPS). HGPS is a rare genetic disorder resulting in phenotypes suggestive of accelerated ageing, including shortened stature, craniofacial disproportion, very thin skin, alopecia and osteoporosis, with death in the early teens predominantly due to atherosclerosis[1]. However, recent reports suggest that developmental abnormalities may also be important in HGPS[1,2]. Here we describe the derivation of mice carrying an autosomal recessive mutation in the lamin A gene (*Lmna*) encoding A-type lamins, major components of the nuclear lamina[3]. Homozygous mice display defects consistent with HGPS, including a marked reduction in growth rate and death by 4 weeks of age. Pathologies in bone, muscle and skin are also consistent with progeria. The *Lmna* mutation resulted in nuclear morphology defects and decreased lifespan of homozygous fibroblasts, suggesting premature cell death. Here we present a mouse model for progeria that may elucidate mechanisms of ageing and development in certain tissue types, especially those developing from the mesenchymal cell lineage.

The *Lmna* gene encodes the A-type lamins, intermediate filament family members that make up the nuclear lamina, a fibrous network underlying the nuclear envelope[3]. Alternative splicing of *Lmna* transcripts gives rise to four proteins: two major products called lamin A and lamin C, and two minor products, laminAΔ10 and lamin C2, the latter being specific to the testis. The A-type lamins interact with B-type lamins, which are encoded by the *Lmnb1* and *Lmnb2* genes, in a largely uncharacterized assembly process to form the nuclear lamina. The A-type lamins are developmentally regulated, whereas at least one B-type lamin is expressed in every cell type at all developmental stages. Embryonic stem cells, cells of the early embryo and haematopoietic stem cells do not express *Lmna*; however, derivatives of these cells do express *Lmna* during development, suggesting a role for *Lmna* in terminal differentiation[4]. In addition to controlling interphase nuclear morphology, the nuclear lamina also functions in selective retention of proteins in the inner nuclear membrane, chromatin organization, DNA replication and gene expression[5,6]. A role for A-type lamins in regulating gene expression is further supported by interactions with a growing number of transcription factors, for example, Rb[7] and GCL indirectly through emerin[8].

The indispensable role of lamins in these diverse and fundamental processes may account for their association with a growing list of human diseases. Laminopathies can be divided loosely into two categories: those affecting striated muscle and those with phenotypes affecting adipose tissue and bone. Diseases of striated muscle caused by mutations in the *Lmna* gene are the autosomal dominant form of Emery–Dreifuss muscular dystrophy (AD-EDMD), limb girdle muscular dystrophy 1B (LGMD1B) and dilated cardiomyopathy with conduction system disease (DCM–CD). A single recessive mutation in *Lmna* has also been implicated in Charcot–Marie–Tooth syndrome type 2B1 (CMT2B1), a peripheral neuropathy with muscle weakness and wasting. Dunnigan's familial partial lipodystrophy (FPLD) and mandibuloacral dysplasia (MAD), disorders primarily resulting in loss and redistribution of white adipose tissue, are also associated with mutations in *Lmna*. Hyperlipidaemia, insulin resistance and diabetes are common in FPLD and MAD patients, and bone defects in MAD patients include craniofacial abnormalities, osteolysis of terminal digits and hypoplasia of clavicles[9]. Many clinical observations of MAD patients are also seen in progeria patients[10], suggesting that the two disorders may be allelic. Although we do not understand why mutations in *Lmna* cause such a wide array of phenotypes, the continued discovery of phenotypic overlap between some of these diseases indicates that they may represent a spectrum of related disorders rather than separate diseases. The present description of progeroid symptoms associated with $Lmna^{L530P/L530P}$ mutant

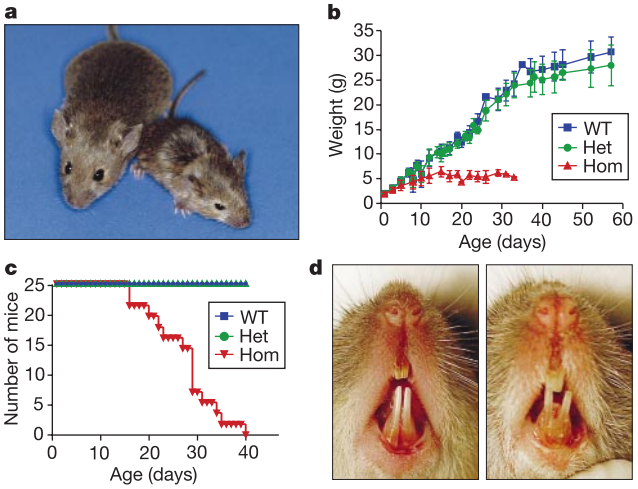

Figure 1 $Lmna^{L530P/L530P}$ homozygous mice exhibit severely retarded growth and die early. **a**, The smaller $Lmna^{L530P/L530P}$ mouse weighed 5.37 g; the littermate (21.88 g) was wild type. **b**, Mutants failed to thrive, showing marked growth reduction as early as 4 days after birth. Mice were weighed every 2–3 days for 58 days. $n = 8$ mutant (Hom, red), 10 wild-type (WT, blue) and 14 heterozygotes (Het, green) mice. **c**, Heterozygotes (green) can live as long as wild-type littermates (blue). Mutants ($n = 25$, red) died by 38 days. **d**, In 50% of mutant mice, we observed abnormal dentition in the lower jaw. A heterozygous littermate is on the left.

mice represents one of the most severe extremes in such a spectrum of laminopathies.

In an effort to create a mouse model for AD-EDMD, we introduced a nucleotide base change into the *Lmna* gene, directing a substitution of proline for leucine at residue 530 (L530P)[11]—a mutation that causes AD-EDMD in humans. Although mice heterozygous for this point mutation do not show signs of muscular dystrophy and have been overtly normal up to 6 months of age, mice homozygous for the mutation (*Lmna*$^{L530P/L530P}$ mice) showed phenotypes markedly reminiscent of symptoms observed in progeria patients. Homozygous *Lmna*$^{L530P/L530P}$ mice are indistinguishable from their littermates at birth, but within 4–6 days develop severe growth retardation, dying within 4–5 weeks (Fig. 1a–c). Progeria patients are unremarkable at birth, but by 2 years of age develop severe growth retardation resulting in shortened stature, and the mean age of death is 12–15 years. Homozygous *Lmna*$^{L530P/L530P}$ mice showed a slight waddling gait, suggesting immobility of joints. Similarly, progeria patients often adopt a 'horse-riding stance' with wide, shuffling gait due to joint stricture[12]. Other progeroid features of *Lmna*$^{L530P/L530P}$ mice include micrognathy and abnormal dentition[12]—in approximately half of the mutants a gap was observed between the lower two incisors, which also appeared yellowed (Fig. 1d). Such tooth gaps and discoloration were not observed in age-matched wild-type or heterozygous mice. Mutant mice continue to feed and defecate until death, and gonadal fat pads are present, suggesting that insufficient food consumption did not cause the decreased growth rate. On suspension by their tails, homozygous mutant mice did not clasp their hind legs, suggesting a normal peripheral motor response. No obvious abnormalities in social behaviour or grooming were noted in the mutant mice. Mentation, IQ and personality are normal in progeria patients[12,13].

Pathology of the heart, skin, skeletal muscle and bone of 4-week-old homozygous *Lmna*$^{L530P/L530P}$ mice suggested developmental defects consistent with progeroid phenotypes (Fig. 2). The most obvious sign of premature ageing occurred in the skin of mutant mice (Fig. 2e, f), which showed an epidermal layer thickened by regions of hyperkeratosis, thinning of the underlying dermis, atrophy of the accompanying muscle, and a complete absence of the subcutaneous fat layer. Increased deposits of collagen, similar to scleroderma, were observed in skin sections stained with Masson's trichrome. A decreased density of hair follicles observed in mutant skin sections may correlate to the alopecia observed in progeria patients; reduced numbers of eccrine and sebaceous glands were also observed in mutants. Mild to moderate degeneration mixed with hypoplasia and/or atrophy of both heart and skeletal muscle

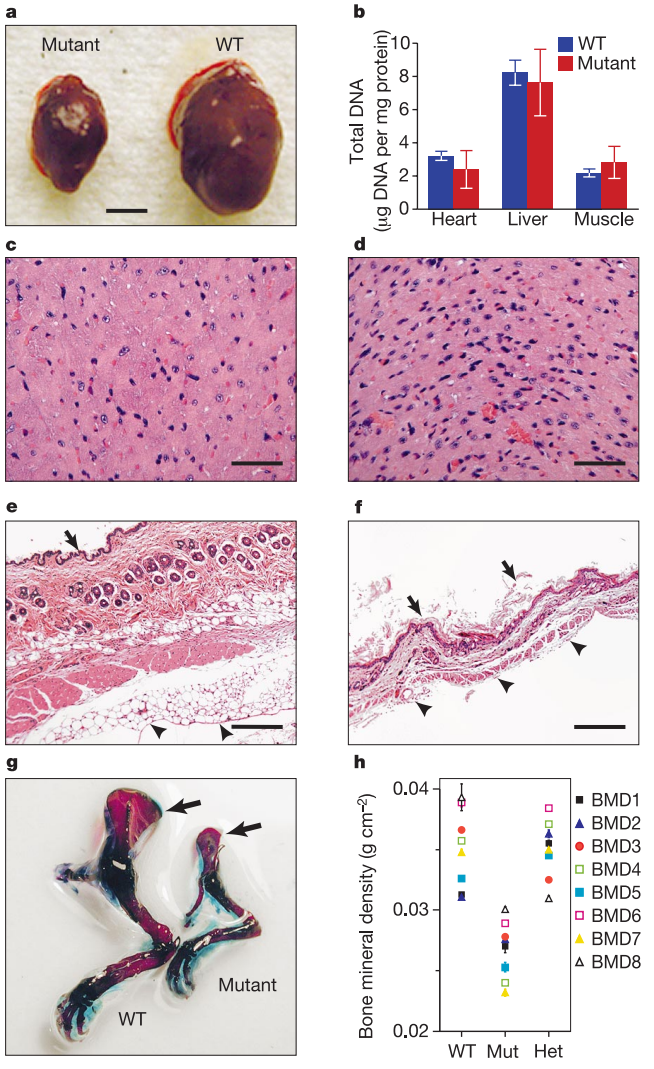

Figure 2 Tissue pathology in *Lmna*$^{L530P/L530P}$ homozygous mutant mice. **a**, The hearts of *Lmna*$^{L530P/L530P}$ mice (left) are smaller than age-matched wild-type hearts (right). Scale bar, 2 mm. **b**, Similar quantities of DNA were found in mutant and wild-type organs. **c**, **d**, Hearts of *Lmna*$^{L530P/L530P}$ mice (**d**) show smaller myocytes than hearts from wild-type mice (**c**). **e**, **f**, Skin from wild-type (**e**) and mutant (**f**) mice. Arrows indicate epidermis, with hyperkeratotic regions in the mutant. Arrowheads indicate subcutaneous fat, of which there is an almost complete absence in the mutant. **g**, Skeletal preparations of wild-type and mutant mice revealed malformed, thin scapulae in *Lmna*$^{L530P/L530P}$ mice. **h**, Bone mineral contents (g cm^{-2}) of wild-type, heterozygote and mutant mice are shown. $n = 8$ per genotype.

Table 1 **Comparison of HGPS phenotypes in human and *Lmna*$^{L530P/L530P}$ mouse**

Human	Mouse
Severe growth retardation	Severe growth retardation
Short stature; failure to thrive	Short stature; failure to thrive
Mean death at 12–15 years	Death at 4–5 weeks
Craniofacial disproportion; micrognathy	Micrognathy
Abnormal dentition	Abnormal dentition
Very thin skin; loss subcutaneous fat	Loss of subcutaneous fat
Decreased eccrine, sebaceous glands	Decreased eccrine, sebaceous glands
Scleroderma	Increased collagen deposition in skin
Alopecia, onset at about 1 year	Decreased hair follicle density
Hyperkeratosis in some patients	Hyperkeratosis
Bone hypoplasia and resorption; osteoporosis	Decreased bone density; thin trabeculae
Hypoplasia/resorption of clavicles	Malformation of scapulae
Resorption of hip-girdle joints; shuffling gait	Waddling gait
Congestive heart failure; decrease in vascular smooth muscle	Heart pathology; subtle changes consistent with pulmonary hypertension
Incomplete sexual maturation	Hypogonadism
No consistent dyslipidaemia	Normal TTG and FFA; low cholesterol
Hypoplastic facial bones	Not determined
Thin diaphyses	Thinner femur; other diaphyses not studied
Osteolysis of terminal digits	None observed
Protruding ears; prominent eyes	Protruding ears
Myocardial fibrosis	Increased cardiac collagen and fibrocyte number
Atherosclerosis	No obvious defects in aorta, small vessels
Poor muscle development; atrophy	Poor muscle development and/or atrophy

Online Mendelian Inheritance in Man (OMIM) cites HGPS cases from two families in which consanguineous siblings were affected with progeroid syndrome, suggesting possible autosomal recessive inheritance. However, many HGPS patients arise from a non-consanguineous union, suggesting an autosomal dominant mode of inheritance. Both modes of inheritance may be possible. *Lmna*$^{L530P/L530P}$ mice are consistent with the autosomal recessive inheritance pattern. TTG, total triglycerides; FFA, free fatty acids.

also occurred in mutant animals. Mutant mice had significantly smaller hearts (Fig. 2a) with myocytes smaller than their wild-type counterparts (Fig. 2c, d). The amount of DNA in known weights of heart tissue was unchanged in mutants, suggesting that the smaller mutant hearts had the same number of cells as wild-type hearts (Fig. 2b). Counts of fibrocyte versus myocyte nuclei in mutant and wild-type hearts indicated that there were 2.6 fibrocytes per myocyte in wild-type hearts, but 4.1 fibrocytes per myocyte in mutant hearts. Although the total number of cells may be equivalent in mutant and wild-type hearts, there appeared to be fewer myocytes in mutant tissue with a compensatory increase in the fibrocyte population. Although not profound, a slight increase in extracellular collagen, indicative of degeneration, was noted in mutant hearts by Masson's trichrome staining (data not shown). Hypoplasia and/or atrophy of oesophageal muscles and myocardiocytes in homozygous *Lmna*$^{L530P/L530P}$ mice suggested either incomplete development or loss of muscle mass in these tissues. Mild to moderate degeneration of other skeletal muscles, including pharyngeal, paravertebral, shoulder, hip, tibia, radius, femur, humerus and tongue, was also observed. However, dystrophic features such as centrally located nuclei and muscle fibres of varying diameter were not observed, ruling out muscular dystrophy, a prominent feature in *Lmna*-null mice[14].

Bone sections from 4-week-old mutant mice showed a decreased number and size of trabeculae, and a decrease in cortex width of vertebrae and femur, consistent with osteoporosis. In 50% of mutant mice surveyed, at least one scapula appeared to be smaller, thinner and misshapen compared with age-matched controls (Fig. 2g), suggesting incomplete development of the shoulder blade. Such defects in a quadruped where scapulae experience more perpendicular stress than the clavicle may correlate with clavicular malformation in MAD and progeria patients. The xiphisternum, formed of cartilage at the lower front midline of the rib cage, also appeared smaller in mutant animals in relation to overall ribcage size. No osteolysis of terminal digits was observed. Densitometry scanning of whole mice indicated a decrease in total bone mineral density of 25–30% in mutant animals compared with wild-type or heterozygous littermates (Fig. 2h). Taken together these results suggest either a premature loss of bone mass or the incomplete development of the skeleton in mice homozygous for *Lmna*$^{L530P/L530P}$, features prominent in patients with HGPS[2]. Consistent with several case histories of progeria subjects[12,15], juvenile testes and ovaries were observed in *Lmna*$^{L530P/L530P}$ mice, indicating incomplete gonadal development. Total necropsy of the animals revealed no incidence of tumours or gross organ deficiencies. A comparison of progeroid phenotypes and those of *Lmna*$^{L530P/L530P}$ mice is summarized in Table 1.

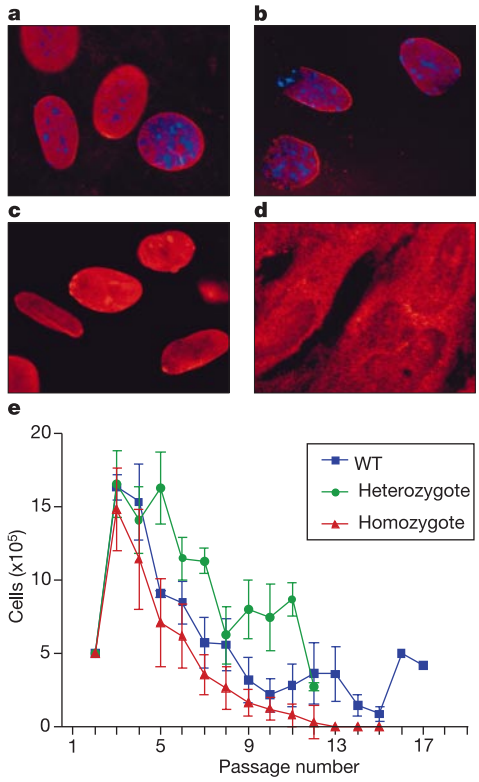

Figure 3 Homozygous *Lmna*$^{L530P/L530P}$ fibroblasts showed nuclear envelope abnormalities and decreased lifespan. **a**–**d**, Indirect immunofluorescence for lamin A (**a** and **b**) or lamin C (**c**, **d**) showed localization of A-type lamins in wild-type (**a**, **c**) or homozygous mutant (**b**, **d**) primary MEFs. 4,6-Diamidino-2-phenylindole counterstaining is shown in blue (**a**, **b**). **e**, Continuous passage assays show decreased doubling capacity and lifespan of *Lmna*$^{L530P/L530P}$ adult fibroblasts isolated from muscle at 4 weeks of age with death of the mutant cells by passage 13. $n = 5$ cell lines for mutant fibroblasts, 5 for heterozygotes, and 6 for wild type.

At the cellular level, nuclear morphology is disrupted in primary mouse embryo fibroblasts (MEFs) from *Lmna*$^{L530P/L530P}$ homozygous embryos, consistent with phenotypes observed in fibroblast cell lines from AD-EDMD, FPLD and DCM patients[16,17]. Discontinuities of the nuclear envelope were seen in 58% of mutant cells (Fig. 3b), whereas only 20% of heterozygous and 5.6% of wild-type cells showed herniations of the nucleus. Areas in which the inner nuclear membrane and outer nuclear membrane appeared to lose contact with each other, resulting in the expansion of the perinuclear space and ballooning of chromatin into a bleb-like structure, may reflect a weakened nuclear lamina in cells expressing *Lmna*$^{L530P/L530P}$. Consistent with a defective nuclear lamina, decreased levels of lamin A were incorporated into the lamina as deduced by indirect immunofluorescence (Fig. 3a, b). Lamin C is completely absent from the nuclear envelope in mutant primary MEFs, and there is an increase in lamin-C-reactive peptides in the cytoplasm, an observation not seen in wild-type cells when stained with the same antibody (Fig. 3c, d). These results suggest that the mutant L530P form of lamin A is competent to assemble at least partially or temporarily in the nuclear lamina, but lamin C is not assembled into the nuclear envelope in *Lmna*$^{L530P/L530P}$ cells. Similar defective lamin A and C incorporation into the lamina was observed in *Lmna*-null primary MEFs when a mutant complementary DNA encoding the L530P variant of *Lmna* was expressed[18]. Western analysis indicated that any A-type lamins translated are unstable, as greatly diminished levels of mutant protein were detected in homozygous mutant cell lines. Cells heterozygous for *Lmna*$^{L530P/L530P}$ had about half the wild-type amount of lamin A and C protein. Consistent with low levels of protein, decreased levels of *Lmna* transcripts were detected by northern analysis in cells from homozygous embryos, suggesting instability of the mutant message, probably due to a splicing defect. Polymerase chain reaction with reverse transcription (RT–PCR) of the region surrounding exon 9, which encodes residue 530, suggests aberrant splicing between exons 9 and 10 in *Lmna*$^{L530P/L530P}$ mice (see Supplementary Information for details).

To determine whether the mutant cells enter senescence earlier than normal as would be expected of prematurely ageing cells, we performed continuous passage assays[19] (Fig. 3e). Wild-type and heterozygous cell lines entered a senescent state at passage 10 to 11; these cells remained viable and attached to the tissue culture surface but did not continue dividing during this period. In contrast, cells homozygous for *Lmna*$^{L530P/L530P}$ stopped dividing and began to disappear from the cultures by passage 8, suggesting that they were dying rather than attaining replicative senescence. Short-term growth characteristics of adult muscle fibroblasts at low cell density were equivalent to wild-type and heterozygous cells at early passage (passage 2), but by passage 6, the mutant cells failed to double over a

10-day course of growth. The premature death of mutant cells suggested that they either had a predetermined shortened lifespan, or that they were unable to respond adequately to the crisis stage that inevitably faces primary mouse cell lines before immortalization. In humans, ageing is associated with telomere shortening; however, we observed no difference in telomere lengths between tissues of wild-type and $Lmna^{L530P/L530P}$ homozygous mice (data not shown).

Thinning of the skin, hypoplasia and degeneration of cardiac and skeletal muscle, osteoporosis, and abnormal dentition in homozygous $Lmna^{L530P/L530P}$ mice are all phenotypes consistent with those seen in progeria patients[1]. Marked growth retardation and shortened lifespan are also hallmarks of progeria. The question of how faithfully progeria simulates natural ageing is, however, controversial, because cataracts, age-related cancers and cognitive decline are not observed in progeria patients[1,2]. $Lmna^{L530P/L530P}$ homozygous mutant mice also failed to show any signs of these age-induced pathologies. One possibility is that progeria is a developmental disease in which there is either accelerated or improper development of certain tissue types, while other tissues are relatively unaffected. The tissues most severely affected in progeria patients and the mutant mice arise from the mesenchymal stem cell lineage, making this a particularly interesting cell lineage for further study in $Lmna^{L530P/L530P}$ mice. Accelerated development and premature death of terminally differentiated mesenchymal cells may account for phenotypes in progeric heart, muscle, bone and subcutaneous adipose tissues. Alternatively, terminally differentiated tissues with defects in the nuclear lamina may be unable to maintain the chromatin organization necessary to preserve a state of terminal differentiation, resulting in dedifferentiation and subsequent redifferentiation into other cell types with age in certain tissues[20,21]. Our preliminary data indicate that homozygous $Lmna^{L530P/L530P}$ muscle myoblasts and fibroblasts readily differentiate into adipocytes, suggesting this latter hypothesis may be valid. Notably, muscles in older individuals show accumulation of fat compared with younger muscle, which could be a result of muscle tissue transdifferentiating into fat during old age[20]. We are further studying these questions in the $Lmna^{L530P/L530P}$ mouse in expectation of learning more about the extent to which differentiation and the loss of cell identity contribute to the ageing process, especially with respect to the phenotypes seen in progeria. □

Methods

Generation of *Lmna* knockin mice

Site-directed mutagenesis of a 1.4-kilobase *Bgl*II–*Bam*HI fragment was performed to introduce a nucleotide polymorphism resulting in the substitution of proline for leucine at amino acid 530 in the *Lmna* gene (see Supplementary Fig. 1A). A neomycin selectable marker flanked by *loxP* sites was inserted in reverse orientation to *Lmna* at the *Sma*I site of intron 9. The targeting vector was linearized and electroporated into W9.5 embryonic stem (ES) cells. Clones selected with neomycin were picked, expanded and screened for recombination. Two recombinant ES lines were injected into C57Bl/6 blastocysts, and chimaeras were bred to produce germline offspring as described[22]. Homozygous, heterozygous and wild-type mice were distinguished based on subjecting an exon 9 PCR product to heteroduplex mobility analysis to discern the presence of the point mutation[23]. To excise the neomycin selectable marker, $Lmna^{L530Pneo/+}$ mice were crossed to mice transgenic for Cre driven by the ubiquitously expressed β1-actin[24]. Progeny were screened for the loss of the neomycin-resistance marker. A PCR-amplified fragment of *Lmna* exon 9 was sequenced from $Lmna^{L530P/L530P}$ mice to verify the presence of the point mutation. All phenotypic characterizations were performed using $Lmna^{L530P/L530P\Delta neo}$ mice. Most of the pathological characterization of $Lmna^{L530P/L530P}$ mice was performed using a mouse line derived from one of the ES cell lines; however, no discernible differences in phenotypes of mice established from the two ES cell lines have been noted.

Characterization of mice

Pathological examination of the mice was performed at approximately 3.5–4 weeks of age. Tissues for histological analysis were fixed in 10% phosphate buffered formalin, dehydrated, cleared, embedded in paraffin, sectioned at 6 μm, and stained with haematoxylin and eosin. Tissues sectioned included heart, pancreas, thyroid, trachea, oesophagus, liver, spleen, thymus, testis, vertebrae with spinal cord, nasal structures, tongue, periscapular fat pad, gonadal fat pat, and muscles from the hip, shoulder, femur, tibia, humerus and radius. To estimate cell number in the heart, total DNA was isolated from wild-type and mutant hearts of four mice of each genotype and normalized for the amount of tissue extracted. Skeletal preparations were performed as described[25]. To quantify bone mineral density, whole mice were scanned using a GE Medical Systems Lunar Piximus densitometry scanner. Three scans per mouse were performed. Error bars indicate standard deviation.

Immunofluorescence

Indirect immunofluorescence was performed on primary MEFs at passage 2 or 3. Anti-lamin A was a gift from B. Burke, and recognizes only lamin A and not lamin C. Anti-lamin C was made to a lamin-C-specific peptide conjugated to keyhole limpet haemocyanin in rabbits. The resulting antiserum was preadsorbed with *Lmna*-null primary MEFs fixed in 3% paraformaldehyde in PBS, and the antiserum recognizes lamin C but not lamin A. Goat anti-rabbit–rhodamine secondary antibodies were used at 1:200 (Biosource International). Continuous passage assays[19] were performed on adult fibroblasts isolated from muscle[26]. For each passage, cells were plated at a density of 5×10^5 and counted every 3.5 days. Standard error of the mean is indicated in error bars.

Received 10 February; accepted 8 April 2003; doi:10.1038/nature01631.

1. Uitto, J. Searching for clues to premature aging. *Trends Endocrinol. Metab.* **13,** 140–141 (2002).
2. de Paula Rodriguez, G. H. *et al.* Severe bone changes in a case of Hutchinson-Gilford syndrome. *Ann. Genet.* **45,** 151–155 (2002).
3. Burke, B. & Stewart, C. L. Life at the edge: the nuclear envelope and human disease. *Nature Rev. Mol. Cell Biol.* **3,** 575–585 (2002).
4. Roeber, R.-A., Sauter, H., Weber, K. & Osborn, M. Cells of the cellular immune and hemopoietic system of the mouse lack lamins A/C: distinction versus other somatic cells. *J. Cell Sci.* **95,** 587–598 (1990).
5. Hutchison, C. Lamins: building blocks or regulators of gene expression? *Nature Rev. Mol. Cell Biol.* **3,** 848–858 (2002).
6. Spann, T. P., Goldman, A. E., Wang, C., Huang, S. & Goldman, R. D. Alteration of nuclear lamin organization inhibits RNA polymerase II-dependent transcription. *J. Cell Biol.* **156,** 603–608 (2002).
7. Ozaki, T. *et al.* Complex formation between lamin A and the retinoblastoma gene product: identification of the domain on lamin A required for its interaction. *Oncogene* **9,** 2649–2653 (1994).
8. Holaska, J. M., Lee, K. K., Kowalski, A. K. & Wilson, K. L. Transcriptional repressor Germ Cell-less (GCL) and Barrier to Autointegration Factor (BAF) compete for binding to Emerin *in vitro*. *J. Biol. Chem.* **278,** 6969–6975 (2003).
9. Worman, H. J. & Courvalin, J. C. The nuclear lamina and inherited disease. *Trends Cell Biol.* **12,** 591–598 (2002).
10. Hoeffel, J. C., Mainard, L., Chastagner, P. & Hoeffel, C. C. Mandibulo-acral dysplasia. *Skeletal Radiol.* **29,** 668–671 (2000).
11. Bonne, G. *et al.* Mutations in the gene encoding lamin A/C cause autosomal dominant Emery-Dreifuss muscular dystrophy. *Nature Genet.* **21,** 285–288 (1999).
12. Ackerman, J. & Gilbert-Barness, E. Hutchinson-Gilford progeria syndrome: a pathologic study. *Pediatr. Pathol. Mol. Med.* **21,** 1–13 (2002).
13. Sarkar, P. K. & Shinton, R. A. Hutchinson-Guilford progeria syndrome. *Postgrad. Med. J.* **77,** 312–317 (2001).
14. Sullivan, T. *et al.* Loss of A-type lamin expression compromises nuclear envelope integrity leading to muscular dystrophy. *J. Cell Biol.* **147,** 913–920 (1999).
15. Lewis, M. PRELP, collagen, and a theory of Hutchinson-Gilford progeria. *Ageing Res. Rev.* **2,** 95–105 (2003).
16. Vigouroux, C. *et al.* Nuclear envelope disorganization in fibroblasts from lipodystrophic patients with heterozygous R482Q/W mutations in the lamin A/C gene. *J. Cell Sci.* **114,** 4459–4468 (2001).
17. Morris, G. E. The role of the nuclear envelope in Emery-Dreifuss muscular dystrophy. *Trends Mol. Med.* **7,** 572–577 (2001).
18. Raharjo, W. H., Enarson, P., Sullivan, T., Stewart, C. L. & Burke, B. Nuclear envelope defects associated with LMNA mutations cause dilated cardiomyopathy and Emery-Dreifuss muscular dystrophy. *J. Cell Sci.* **114,** 4447–4457 (2001).
19. Todaro, G. J. & Green, H. Quantitative studies of the growth of mouse embryo cells in culture and their development into established lines. *J. Cell Biol.* **17,** 299–313 (1963).
20. Taylor-Jones, J. M. *et al.* Activation of an adipogenic program in adult myoblasts with age. *Mech. Ageing Dev.* **123,** 649–661 (2002).
21. Kirkland, J. L., Tchkonia, T., Pirtskhalava, T., Han, J. & Karagiannides, I. Adipogenesis and aging: does aging make fat go MAD? *Exp. Gerontol.* **37,** 757–767 (2002).
22. Stewart, C. L. Production of chimeras between embryonic stem cells and embryos. *Methods Enzymol.* **225,** 823–855 (1993).
23. Upchurch, D. A., Shankarappa, R. & Mullins, J. I. Position and degree of mismatches and the mobility of DNA heteroduplexes. *Nucleic Acids Res.* **28,** E69 (2000).
24. Lewandoski, M., Meyers, E. N. & Martin, G. R. Analysis of Fgf8 gene function in vertebrate development. *Cold Spring Harb. Quant. Biol.* **62,** 159–168 (1997).
25. Lufkin, T. *et al.* Homeotic transformation of the occipital bones of the skull by ectopic expression of a homeobox gene. *Nature* **359,** 835–841 (1992).
26. Sabourin, L. A. *et al.* Reduced differentiation potential of primary MyoD$^{-/-}$ myogenic cells derived from adult skeletal muscle. *J. Cell Biol.* **144,** 631–643 (1999).

Supplementary Information accompanies the paper on **www.nature.com/nature**.

Acknowledgements We thank L. Sewell for technical assistance in our animal facility; D. Haines and D. Smith for help in pathological examination of the mice; H. Wimbrow for assistance in the use of the Piximus densitometer; R. Frederickson for preparation of the figures and B. Burke and B. Howard for discussions.

Competing interests statement The authors declare that they have no competing financial interests.

Correspondence and requests for materials should be addressed to C.L.S. (stewartc@ncifcrf.gov).